




ORIGINAL RESEARCH

Segmental Cardiac Radiation Dose Determines Magnitude of Regional Cardiac Dysfunction

Siddharth J. Trivedi , BSc, BMedSci (Hons), MBBS (Hons); Simon Tang, MBBS, BMedSci; Karen Byth , C.Stat.RSS, PhD; Luke Stefani, BBioMedSci (Hons); Queenie Lo, MBBS (Hons), BSc (Med) (Hons), PhD; James Otton, MBBS, PhD; Michael Jameson, BMedRadPhys (Hons), PhD; David Tran, BAppSc, MBBS, MMed; Vikneswary Batumalai, BSc, MHIthSc, PhD; Lois Holloway, BMedPhys (Hons), PhD; Geoff P. Delaney, MBBS, MD, PhD; Eng-Siew Koh, MBBS; Liza Thomas , MBBS, PhD

BACKGROUND: Subclinical left ventricular dysfunction detected by 2-dimensional global longitudinal strain post breast radiotherapy has been described in patients with breast cancer. We hypothesized that left ventricular dysfunction postradiotherapy may be site specific, based on differential segmental radiotherapy dose received.

METHODS AND RESULTS: Transthoracic echocardiograms were performed at baseline, 6 weeks, and 12 months postradiotherapy on 61 chemotherapy-naïve women with left-sided breast cancer undergoing tangential breast radiotherapy. Radiation received within basal, mid, and apical regions for the 6 left ventricular walls was quantified from the radiotherapy treatment planning system. Anterior, anteroseptal, and anterolateral walls received the highest radiation doses, while inferolateral and inferior walls received the lowest. There was a progressive increase in the radiation dose received from basal to apical regions. At 6 weeks, the most significant percentage deterioration in strain was seen in the apical region, with greatest reductions in the anterior wall followed by the anteroseptal and anterolateral walls, with a similar pattern persisting at 12 months. There was a within-patient dose–response association between the segment-specific percentage deterioration in strain at 6 weeks and 12 months and the radiation dose received.

CONCLUSIONS: Radiotherapy for left-sided breast cancer causes differential segmental dysfunction, with myocardial segments that receive the highest radiation dose demonstrating greatest strain impairment. Percentage deterioration in strain observed 6 weeks postradiotherapy persisted at 12 months and demonstrated a dose–response relationship with radiotherapy dose received. Radiotherapy-induced subclinical cardiac dysfunction is of importance because it could be additive to chemotherapy-related cardiotoxicity in patients with breast cancer. Long-term outcomes in patients with asymptomatic strain reduction require further investigation.

Key Words: breast cancer ■ cardiotoxicity ■ global longitudinal strain ■ LV dysfunction ■ radiotherapy ■ strain echocardiography

Breast cancer is the leading cause of cancer death among women worldwide.¹ Radiotherapy decreases cancer recurrence and improves survival,² and ≈80% of patients with breast cancer receive radiotherapy.³ However, incidental cardiac radiation results in increased long-term cardiac morbidity and mortality, with adverse events observed in a

dose-dependent manner.⁴ Radiation-associated cardiac disease (RACD) has been thought to manifest years or decades after chest radiotherapy.⁵ Diagnosis of RACD is challenging, because presentation is often vague and overlaps with many conditions.⁵

Two-dimensional speckle tracking strain echocardiography tracks myocardial speckles over the

Correspondence to: Professor Liza Thomas, Department of Cardiology, Westmead Hospital, PO BOX 533, Wentworthville, NSW2145, Australia. E-mail: liza.thomas@sydney.edu.au; l.thomas@unsw.edu.au

For Sources of Funding and Disclosures, see page 11.

© 2021 The Authors. Published on behalf of the American Heart Association, Inc., by Wiley. This is an open access article under the terms of the Creative Commons Attribution-NonCommercial-NoDerivs License, which permits use and distribution in any medium, provided the original work is properly cited, the use is non-commercial and no modifications or adaptations are made.

JAHA is available at: www.ahajournals.org/journal/jaha

CLINICAL PERSPECTIVE

What Is New?

- During left breast cancer treatment with radiotherapy, the anterior, anteroseptal, and anterolateral left ventricular walls receive the highest radiotherapy dose.
- Radiotherapy dose received increases from basal to apical regions for all left ventricular walls.
- The greatest reduction in myocardial strain at 6 weeks is in the anterior wall, followed by the anteroseptal and anterolateral left ventricular walls, and changes in strain persist at 12 months; there is a linear within-patient dose–response relationship between radiotherapy dose and deterioration from baseline strain at 6 weeks and 12 months.

What Are the Clinical Implications?

- There is emerging benefit in breast cancer from techniques such as regional nodal radiotherapy, which may result in greater cardiac radiotherapy doses.
- Strain imaging may play a role in the surveillance of patients with breast cancer undergoing radiotherapy.
- This may be particularly useful in the setting of concomitant chemotherapy and may help guide cardioprotective therapy.

Nonstandard Abbreviations and Acronyms

GLS	global longitudinal strain
RACD	radiation-associated cardiac disease

cardiac cycle and provides unique information about global and segmental myocardial deformation.⁶ Global longitudinal strain (GLS) has improved sensitivity and prognostic value compared with left ventricular ejection fraction (LVEF).⁶ Additionally, strain can evaluate segmental LV function, which may be altered despite preservation of overall myocardial function.

In this study of chemotherapy-naïve patients with breast cancer, we hypothesized that radiotherapy has a dose-dependent effect on the heart that can be demonstrated and quantified by speckle tracking strain echocardiography.

METHODS

The data that support the findings of this study are available from the corresponding author upon reasonable request.

Patient Population

Sixty-one female patients with left-sided breast cancer were prospectively recruited from 2 tertiary hospitals (Liverpool and Campbelltown Hospitals) in Sydney, Australia (April 2009–November 2017). Inclusion criteria were chemotherapy-naïve patients with histologically confirmed left-sided breast cancer, treated with breast conservation surgery (lumpectomy) and adjuvant tangential breast radiotherapy with no nodal radiotherapy. Hormonal treatment was administered in patients who were hormone receptor positive. Exclusion criteria were prior chemotherapy or radiotherapy, previous ischemic heart disease, heart failure, or more than mild valvular disease. Written informed consent was obtained from patients with study protocol approved by the area ethics committee (SSWAHS HREC no. ECOO136).

Radiation Technique

A noncontrast, planning computed tomography scan was performed on all patients pretreatment. Breast radiotherapy was performed with tangential photon beams with minimization of heart volume within the radiotherapy field, however, without shielding the heart if this compromised the target volume coverage. In particular, these patients were treated before the introduction of deep inspiration breath hold techniques, which have subsequently been introduced for patients undergoing tangential radiotherapy for left-sided breast cancer.⁷ Patients were treated supine on a breast board with 6 MV and/or a mix of 6 and 18 MV photons. The radiotherapy treatment regimen was either standard (50 Gy in 25 daily fractions) or hypofractionated (42.4 Gy in 16 daily fractions) protocols, with or without a boost to the surgical cavity.

Radiation Dose–Function Relationship

Our methods have been described in detail previously.⁸ In brief, all patients were simulated in a semirecumbent supine position, immobilized in a breast jig and vacuum bag. Routine planning computed tomography scans undertaken on a Phillips Brilliance Big Bore 16 slice computed tomography scanner (Amsterdam, Netherlands) were used for cardiac delineation (non-contrast and non-ECG-gated), acquired at 2-mm slice thickness. The imaging data sets were transferred to the Oncentra Brachytherapy software v4.5.2 (Elekta, Stockholm, Sweden), and reformatted into cardiac planes to generate the cardiac short axis, 2-chamber and 4-chamber apical views. Rotation was applied to only 1 plane at a time. The cardiac chambers, valves, and 18 segments of the LV as per the American Heart Association (AHA) model⁹ were then contoured in these planes using Radiation Therapy Oncology Group consensus guidelines.¹⁰ The whole heart and coronary

arteries were contoured in the standard orthogonal (axial) plane. Basal, mid, and apical LV regions were formed by summing American Heart Association segments 1–6, 7–12, and 13–18, respectively (Figure 1A).⁹ Segments were also combined by the 6 LV walls, namely, anterior (segments 1, 7, and 13), anteroseptal (segments 2, 8, and 14), inferoseptal (segments 3, 9, and 15), inferior (segments 4, 10, and 16), inferolateral (segments 5, 11, and 17), and anterolateral (segments 6, 12, and 18) (Figure 1B). Contours were performed by a single observer (S.T.), and the first 10 cases were reviewed and verified by 1 of the study cardiologists (J.O.). Additionally, the contour segmentation was consistent with previously published studies.¹¹ This radiotherapy structure data set was imported into Pinnacle v9.10 where dose was calculated. MIM software v6.77 (Mim Software Inc., Cleveland, OH) was used to read out dosimetric data. The radiotherapy doses reported are as predicted by the treatment planning system. In this study, absolute radiation doses were used, with no EQD2 conversions used to normalize the hypofractionated doses. Only mean radiation doses to each of the 18 LV segments were used for analysis. A spatial depiction of the radiation beam and the LV is presented in Figure 2.

Echocardiographic Examination

A comprehensive transthoracic echocardiogram was performed at baseline (preradiotherapy), 6 weeks and 12 months postradiotherapy, by experienced personnel (Vivid 7 or E9 systems, General Electric, Horten, Norway), and frame-rate optimized (≥ 60 frames per second) images from the apical 2-, 3-, and 4-chamber views were obtained for offline analysis.

Two-dimensional, Doppler, and M-mode measurements were also performed.

LV systolic function was evaluated by LVEF, using the Simpson’s biplane method of discs.⁹ Two-dimensional speckle tracking strain echocardiography strain analysis was performed using dedicated software (Echopac 201; GE,) to measure LV GLS from apical-4, -2, and 3-chamber strain traces. An average of 3 cardiac cycles was analyzed for each view. We previously have not observed a significant change in circumferential strain 6 weeks postradiotherapy,¹² and hence circumferential strain was not analyzed. Radial strain was also not evaluated because it has significant interobserver variability,⁶ limiting its clinical utility. Biplane maximum left atrial volume was measured using the method of discs.⁹

Inter- and intraobserver reproducibility for GLS was performed on 15 randomly selected patients. Measurements were performed by 2 blinded observers; measurements were repeated by 1 observer after 4 weeks.

Statistical Analysis

Statistical analysis was performed using IBM SPSS statistics (version 25; IBM Corporation, Armonk, NY) and S-PLUS (version 8) (SolutionMetrics, Sydney, Australia). Continuous variables are summarized as mean \pm SD, and categorical variables as frequencies and percentages. Linear mixed-effects models were used to investigate the joint effects of LV wall (6-level factor comprising anterior, anteroseptal, inferoseptal, inferior, inferolateral, and anterolateral) and region (3-level factor comprising basal, mid, and apical) on the percentage deterioration in strain observed for the 18-segment American

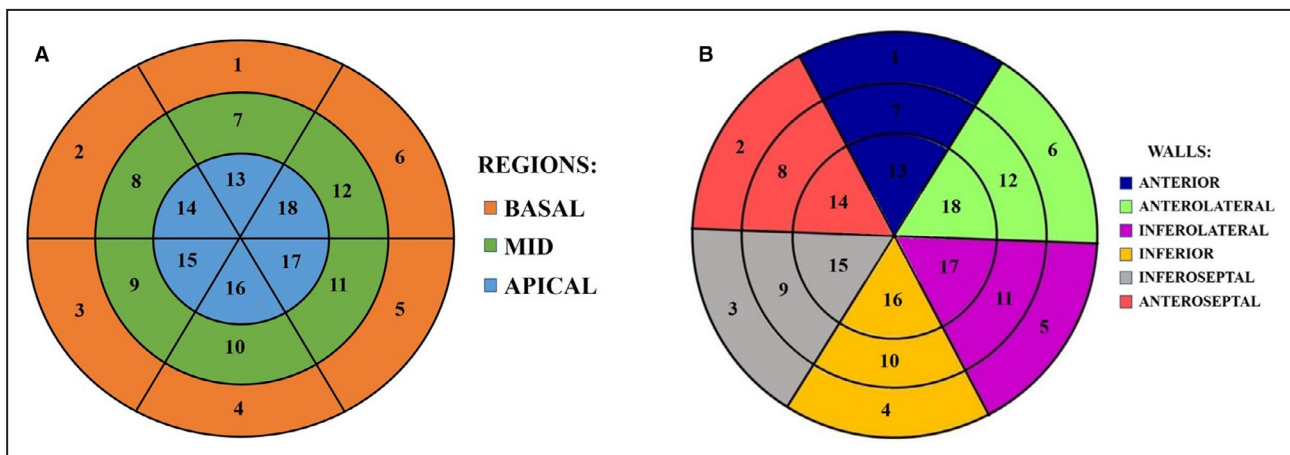


Figure 1. LV regions and walls.

A, Diagrammatic representation of basal, mid, and apical regions. Eighteen segments as per AHA model are shown.⁹ Segments 1–6 formed the basal region (orange), segments 7–12 the mid region (green), and segments 13–18 the apical region (blue). **B**, Diagrammatic representation of 6 LV walls. Eighteen segments as per AHA model are shown.⁹ Each wall is depicted by a color; segments 1, 7, and 13 formed the anterior wall, segments 2, 8, and 14 the anteroseptal wall, and so on. AHA indicates American Heart Association; and LV, left ventricular.

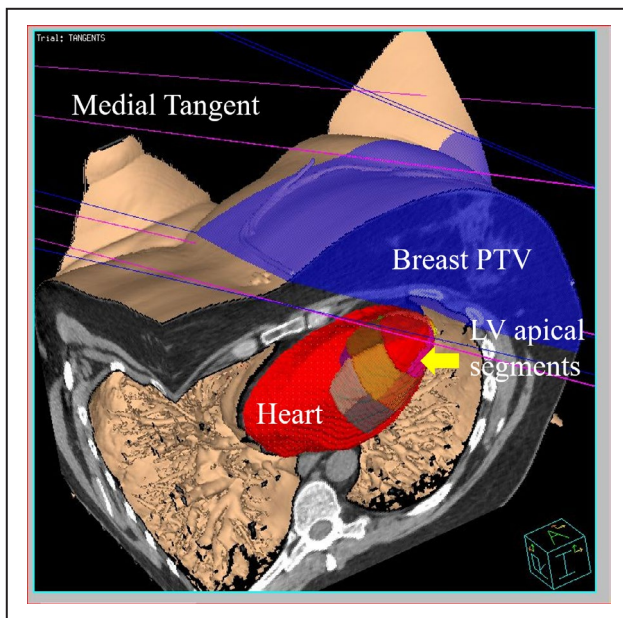


Figure 2. Spatial relationship of LV and radiation beam.

A 3-dimensional reconstruction of a sample patient is shown. The blue volume represents breast PTV. Medial and lateral tangential radiation beams can be seen covering this volume. The entire heart is outlined in red. LV segments are displayed, with the apical and anterior segments being within the radiation field. LV indicates left ventricular; and PTV, planning target volume.

Heart Association model from baseline to 6 weeks and from baseline to 12 months. The percentage deterioration from baseline strain at 6 weeks was calculated as $100 \times (\text{strain}_{\text{baseline}} - \text{strain}_{\text{6weeks}}) / \text{strain}_{\text{baseline}}$, and similarly at 12 months. In these models, patient ID was used as the group identifier, LV wall and region were fitted as both fixed and random effects with a general symmetric covariance structure, and their 2-way interaction as a fixed effect. Linear mixed-effects models were also used to investigate the joint effects of region and log of the radiation dose, on the percentage deterioration from baseline strain observed at 6 weeks and at 12 months. In these models, the continuous variable, log radiation dose (to base 2), was fitted as a random and as a fixed effect, and the 2-way interaction between region and \log_2 (radiation dose) was fitted as a fixed effect. Diagnostic residual plots were used to check the adequacy of the fitted models. Two-tailed tests with significance level of 5% were used throughout. Inter- and intraobserver reproducibility for GLS were reported as coefficients of repeatability.

RESULTS

Patient Population and Radiotherapy Dose

Sixty-one female patients with breast cancer were prospectively enrolled and underwent serial echocardiograms

(preradiotherapy, 6 weeks and 12 months postradiotherapy); all patients were in sinus rhythm. Baseline patient demographics and cardiovascular risk factors are presented in Table 1.

Mean dose to each of the 18 segments, to the basal, mid, and apical regions, and to each of the six LV walls is presented in Table 1. Radiotherapy dose was highest in the apical region, with anterior, anteroseptal, and anterolateral apical segments receiving the highest dose. Figure 3A illustrates the mean radiotherapy dose (on a logarithmic scale) with 95% CI for a given region by LV wall. Inferolateral and inferior walls received the least radiotherapy dose, and the radiotherapy dose received increased from basal to mid to apical regions ($P < 0.001$ for all pairwise comparisons between regions within a LV wall).

Radiotherapy Dose and Echocardiographic Parameters

Echocardiographic parameters at the 3 time points are summarized in Table 2; strain data are presented as individual segmental strain and of LV regions and walls.

LV volumes and EF were normal at baseline and at 12-month follow-up, with no significant within-patient change in LVEF. However, mean end-diastolic volume and end-systolic volume progressively increased from baseline.

Figure 3B illustrates the percentage deterioration from baseline strain at 6 weeks (with 95% CI) for basal, mid, and apical regions for the 6 LV walls. Across all walls, the apical region demonstrated the most significant reduction in strain. The anterior, anteroseptal, and anterolateral walls demonstrated a reduction in strain across the basal, mid, and apical regions while inferolateral and inferior walls demonstrated no reduction in strain.

The percentage deterioration from baseline strain at 12 months demonstrated a pattern similar to that at 6 weeks, with an attenuation in strain reduction (Figure 3C).

Figure 4A illustrates the segmental strain at baseline, and at 6 weeks- and 12 months-postradiotherapy as a composite of data from all patients. The mean radiation dose in each segment, along with the percentage deterioration from baseline strain at 6 weeks and 12 months, as a composite of data from all patients, is depicted in Figure 4B.

Regional Effects

There was a significant interaction between the effects of region and LV walls on the percentage deterioration from baseline strain at 6 weeks ($P < 0.001$) and 12 months ($P = 0.007$). Therefore, separate models were fitted in each of the 6 LV walls to assess the effect of region and quantify the difference between

Table 1. Patient Characteristics and Clinical Data With Radiation Dose by AHA Segment and by Region and by LV Wall

Parameter	Mean±SD / Frequency (%)
Age, y	59.6±8.5
Body mass index, kg/m ²	27.4±6.7
Systolic blood pressure, mm Hg	134±14
Diastolic blood pressure, mm Hg	78±9
Smoking, %	18 (30)
Diabetes mellitus, %	12 (20)
Hypertension, %	28 (46)
Dyslipidemia, %	30 (49)
Mean RT dose (Gy)	
By AHA segment	
Basal	
Anterior	2.66±0.40
Anterolateral	2.28±0.40
Inferolateral	1.29±0.31
Inferior	1.59±0.34
Inferoseptal	1.47±0.33
Anteroseptal	2.04±0.38
Mid	
Anterior	8.84±4.32
Anterolateral	5.28±2.42
Inferolateral	2.19±0.46
Inferior	2.60±0.52
Inferoseptal	2.59±0.61
Anteroseptal	4.62±2.09
Apical	
Anterior	31.71±8.72
Anterolateral	21.28±10.04
Inferolateral	6.70±3.60
Inferior	8.76±5.33
Inferoseptal	10.55±5.43
Anteroseptal	23.35±9.69
By Region	
Basal	1.89±0.60
Mid	4.35±3.20
Apical	17.06±11.75
By LV wall	
Anterior	14.40±13.72
Anterolateral	9.61±10.26
Inferolateral	3.40±3.16
Inferior	4.32±4.43
Inferoseptal	4.87±5.13
Anteroseptal	10.00±11.10

AHA indicates American Heart Association; LV, left ventricular; and RT, radiotherapy.

basal and mid, and between basal and apical regions; Table 3 summarizes the pairwise comparisons of within-subject changes at 6 weeks and at 12 months.

The largest differences in percentage deterioration from baseline strain were seen between apical and basal regions in all 6 LV walls at both 6 weeks and 12 months, with differences most apparent in the anterior and anteroseptal LV walls.

Figure 5 presents scatterplots of the percentage deterioration from baseline strain at 6 weeks versus the \log_2 (radiation dose) for 4 patients, demonstrating a clear dose–response effect, which is approximately linear, when percentage deterioration from baseline strain is plotted against \log_2 (radiation dose). Similar patterns were demonstrated in all patients for both 6-week and 12-month percentage deterioration versus \log_2 (radiation dose) (data not shown). Linear mixed effects models fitted to the full data set found no significant interaction between the effects of region and \log_2 (radiation dose) on the percentage deterioration from baseline strain at 6 weeks ($P=0.373$) or at 12 months ($P=0.249$). Therefore, the interaction term was dropped and only the main effects fitted for each follow-up time. Table 4 shows the slope and its SE within each region along with the overall common slope for percentage deterioration from baseline strain versus \log_2 radiation dose at 6 weeks and at 12 months. The slope has a very simple interpretation in these models; it is the percentage deterioration from baseline strain associated with a doubling of the radiation dose. In other words, a doubling in radiation received between 2 segments was associated with an average difference in percentage deterioration from baseline strain at 6 weeks of -5.7% (95% CI -6.4% to -5.0%), $P<0.001$ and at 12 months of -4.4% (95% CI -5.3% to -3.5%), $P<0.001$.

Reproducibility

Inter- (S.J.T. and L.S.) and intraobserver (S.J.T.) coefficients for repeatability for GLS were 2.7 and 1.6, respectively, in 15 randomly selected patients.

DISCUSSION

This study demonstrates detailed dose-related site-specific changes in myocardial strain in the short- to medium-term follow-up of patients with left-sided breast cancer undergoing adjuvant tangential breast or chest wall radiotherapy. We demonstrate that (1) radiotherapy dose is highest in the anterior wall followed by the anteroseptal and anterolateral LV walls, and lowest in the inferolateral and inferior walls, (2) radiotherapy dose received increases from basal to apical regions for all LV walls, (3) the greatest reductions in myocardial strain at 6 weeks were in the anterior wall followed by the anteroseptal and anterolateral walls and persist at 12 months, and (4) there is a within-patient dose–response relationship between radiotherapy dose and percentage deterioration from baseline strain at 6 weeks and 12 months.

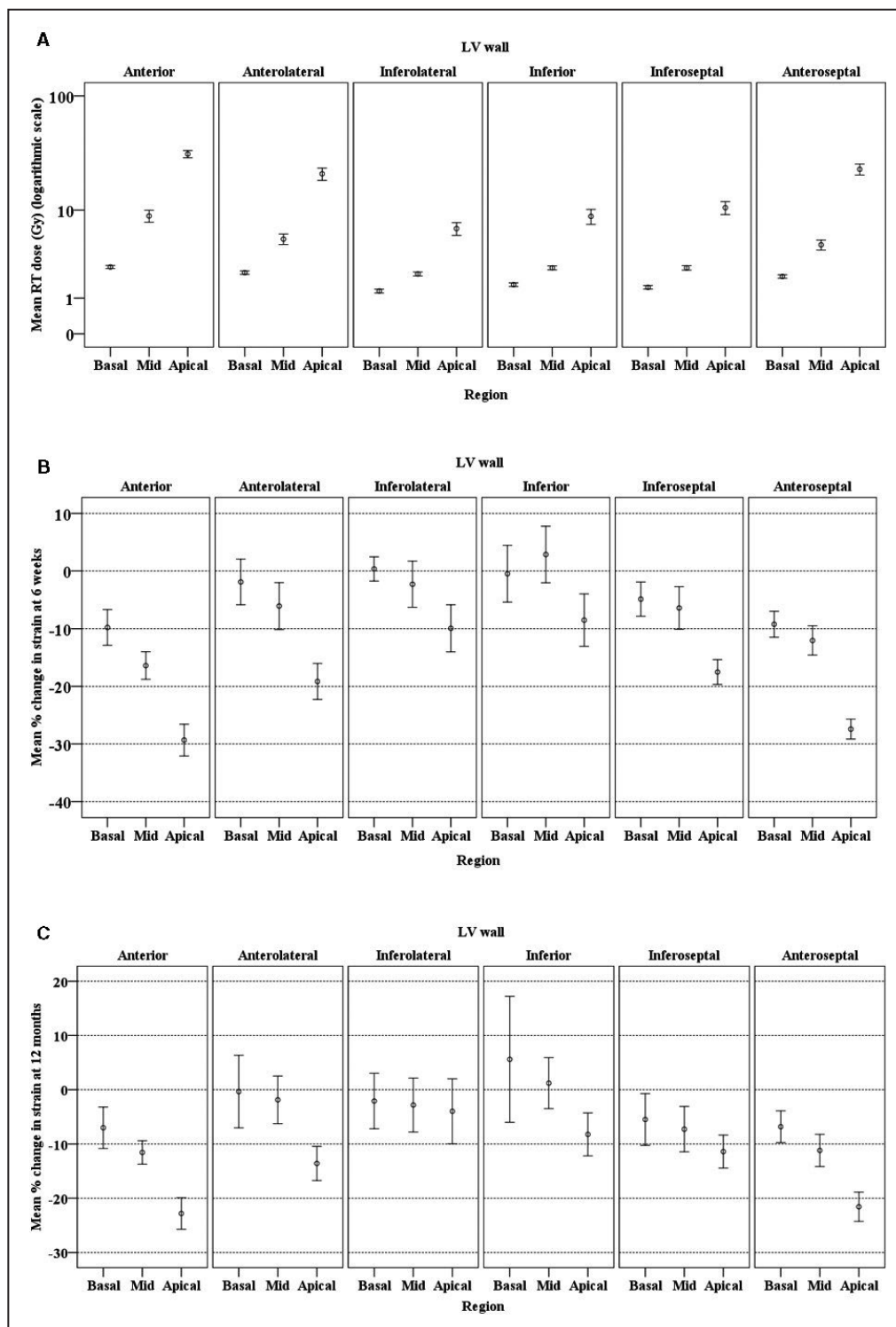


Figure 3. Radiation dose and percentage deterioration from baseline strain.

A, The mean radiation dose (logarithmic scale) with 95% CI for a given region by LV wall. RT dose was the highest in the apical region, with apical anterior, anteroseptal, and anterolateral segments receiving the highest RT dose. **B**, Percentage deterioration from baseline strain at 6 weeks with 95% CI for a given region by LV wall. Across all walls, the apical region demonstrated the most significant reduction in strain. Within all 3 regions, the anterior and anteroseptal segments demonstrated a reduction in strain. Within the basal and mid regions, the inferolateral and inferior segments demonstrated no significant reduction in strain. **C**, Percentage deterioration from baseline strain at 12 months with 95% CI for a given region by LV wall. A pattern similar to that at 6 weeks was observed, with an attenuation in the size of the reduction. LV indicates left ventricular; and RT, radiotherapy.

Table 2. Echocardiographic Parameters at Baseline and Follow-Up Time Periods

Parameter	Baseline (pre-RT)	6 wks Post RT	12 mo Post RT	P Value (Repeated Measures ANOVA)
Systolic function				
Biplane EDV, mL	72.1±21.2	78.6±19.0	86.5±17.2	<0.001
Biplane ESV, mL	26.5±8.3	28.6±9.1	32.5±8.6	0.003
Ejection fraction (%)	61.4±4.8	61.8±4.6	61.2±4.5	0.64
Diastolic parameters				
Peak E, m/s	0.71±0.5	0.69±0.4	0.70±0.5	0.87
Peak A	0.75±0.13	0.77±0.15	0.79±0.11	0.06
Average e', cm/s	8.0±2.0	7.9±1.9	8.1±2.0	0.51
E/A ratio	1.01±0.3	1.00±0.2	0.91±0.2	0.03
DT, ms	205±9	216±10	221±11	0.17
Strain (%)				
Global longitudinal strain	-21.5±1.8	-19.2±2.0	-18.5±1.7	<0.001
By AHA segment				
Basal				
Anterior	-17.28±3.14	-15.40±2.76	-16.11±3.39	
Anterolateral	-16.32±3.17	-15.66±2.34	-15.64±2.92	
Inferolateral	-19.44±4.18	-20.04±3.59	-19.05±4.57	
Inferior	-17.00±3.47	-16.75±3.34	-16.91±4.22	
Inferoseptal	-18.69±4.16	-17.82±3.68	-17.99±4.51	
Anteroseptal	-18.59±4.38	-17.06±4.13	-17.46±4.34	
Mid				
Anterior	-21.68±3.92	-18.17±3.49	-19.42±4.81	
Anterolateral	-18.71±2.79	-17.43±3.00	-18.05±3.18	
Inferolateral	-19.62±3.96	-19.77±3.88	-18.96±4.13	
Inferior	-18.93±3.31	-19.14±3.11	-18.87±3.63	
Inferoseptal	-19.31±3.80	-17.67±3.10	-18.23±4.11	
Anteroseptal	-19.29±4.09	-17.09±3.87	-17.23±3.91	
Apical				
Anterior	-26.47±5.91	-19.11±4.37	-20.82±6.57	
Anterolateral	-27.13±3.69	-21.80±4.47	-23.33±5.15	
Inferolateral	-23.23±5.97	-21.40±5.19	-21.89±4.94	
Inferior	-26.69±4.43	-24.08±5.16	-24.46±4.84	
Inferoseptal	-25.66±4.22	-20.69±3.80	-22.63±4.81	
Anteroseptal	-24.97±3.63	-18.26±3.06	-19.77±4.52	
By Region				
Basal	-17.89±3.91	-17.12±3.67	-17.19±4.17	
Mid	-19.59±3.78	-18.21±3.53	-18.46±4.03	
Apical	-25.69±4.88	-20.89±4.76	-22.15±5.37	
By LV wall				
Anterior	-21.81±5.83	-17.56±3.91	-18.78±5.44	
Anterolateral	-20.72±5.65	-18.30±4.25	-19.01±5.03	
Inferolateral	-20.76±5.07	-20.40±4.31	-19.97±4.73	
Inferior	-20.87±5.62	-19.99±5.00	-20.08±5.31	
Inferoseptal	-21.22±5.13	-18.72±3.78	-19.61±4.95	
Anteroseptal	-20.95±4.94	-17.47±3.73	-18.15±4.39	

AHA indicates American Heart Association; DT, deceleration time; EDV, end diastolic volume; ESV, end systolic volume; LV, left ventricular; and RT, radiotherapy.

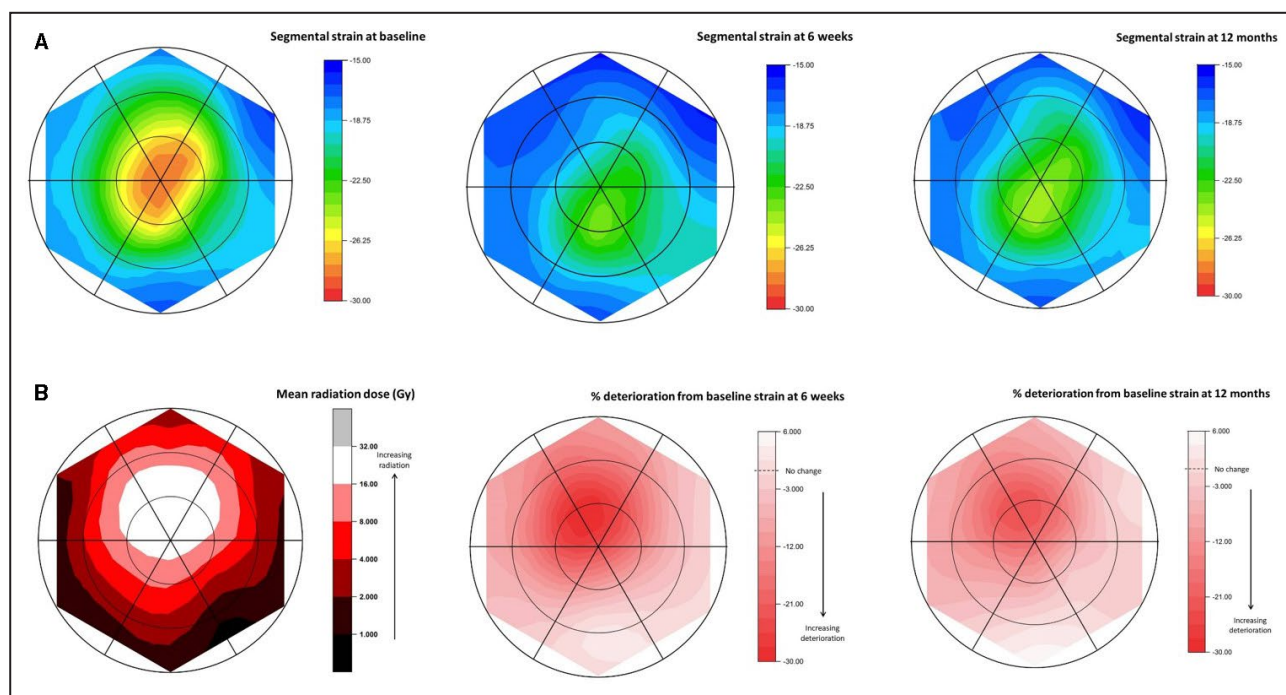


Figure 4. Segmental strain over time.

A, Segmental strain at baseline, and at 6 weeks- and 12 months-post RT as a composite of data from all patients. Areas of best strain are colored orange (in central apical region at baseline). Graded transition (as indicated by the vertical color bar key) towards blue tones indicate worsening strain. The same color scale has been used at each time point to facilitate comparison. **B**, Segmental radiation dose and percentage deterioration from baseline segmental strain at 6 weeks- and 12 months-post-RT as a composite of data from all patients. The RT dose color map uses a log₂ scale, with the white area receiving the highest RT dose, and progressively darker areas receiving progressively lower RT doses. The percentage deterioration from baseline strain is worst in deep red areas, diminishing to no deterioration in white areas. There is a clear correspondence between segments receiving the largest RT dose and segments demonstrating the worst percentage deterioration from baseline strain. RT indicates radiotherapy.

A strength of our study was the inclusion of chemotherapy-naïve patients with left-sided breast cancer, without previous cardiac disease, which permitted precise assessment of the effects of radiotherapy without

the confounding effects of chemotherapy or previous myocardial involvement. With systematic cardiac segmentation, we could evaluate the cardiac subvolume dosimetry and correlation with segmental alteration in strain.

Table 3. Within-Patient Pairwise Comparisons of Basal Versus Mid and Apical Percentage Changes in Strain From Baseline at 6 weeks and 12 months by LV Walls

Time	LV Wall	Mid-Basal			Apical-Basal		
		Mean (%)	SE	P Value	Mean (%)	SE	P Value
6 wks	Anterior	-6.61	1.72	<0.001	-19.54	2.08	<0.001
	Anterolateral	-4.18	1.89	0.029	-17.27	2.25	<0.001
	Inferolateral	-2.66	2.02	0.191	-10.31	2.19	<0.001
	Inferior	3.34	1.81	0.068	-8.051	3.39	0.020
	Inferoseptal	-1.54	1.57	0.329	-12.65	1.63	<0.001
	Anteroseptal	-2.83	1.18	0.019	-18.20	1.06	<0.001
12 mo	Anterior	-4.54	1.97	0.023	-15.79	2.18	<0.001
	Anterolateral	-1.52	2.18	0.487	-13.24	3.42	<0.001
	Inferolateral	-0.73	2.24	0.745	-1.88	4.11	0.648
	Inferior	-4.38	4.48	0.330	-13.83	5.86	0.020
	Inferoseptal	-1.80	1.82	0.326	-5.92	2.96	0.048
	Anteroseptal	-4.38	1.18	<0.001	-14.76	1.73	<0.001

LV indicates left ventricular.

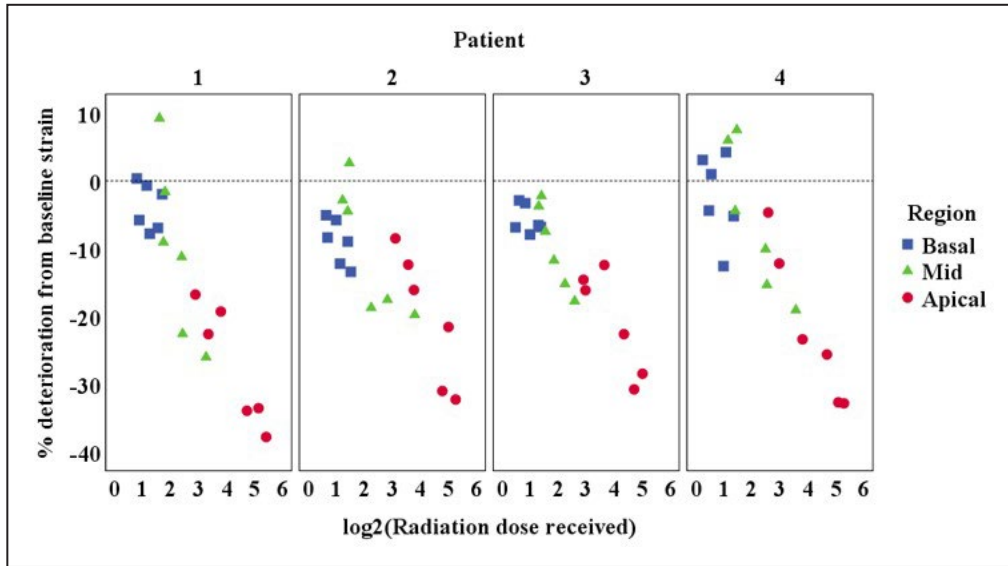


Figure 5. Scatterplots for 4 patients demonstrating the within-subject effect of \log_2 (radiation dose) on percentage deterioration from baseline segmental strain at 6 weeks. A dose–response effect, which is approximately linear, when percentage deterioration from baseline strain is plotted against \log_2 (radiation dose), was demonstrated. Similar patterns were apparent within each patient at both 6 weeks and 12 months.

GLS Postradiotherapy

GLS is a sensitive marker of subclinical LV dysfunction in several conditions, including hypertension, diabetes mellitus, infiltrative cardiomyopathies, and chemotherapy-related cardiotoxicity.⁶ Our group has reported subclinical alterations detected by strain in LV systolic¹² and diastolic function,¹³ persisting at 12 months postradiotherapy.¹⁴ Similar reductions in LV GLS from a few weeks to 14 months after radiotherapy, despite normal LVEF, have been reported.^{15–19} It is unclear, however, whether these changes predict long-term cardiac dysfunction or specific clinical events. However, detecting overt reduction in LVEF after radiotherapy may be too late for treatment.²⁰ A previous study in young adults who received high-dose mediastinal radiotherapy (5–144 months prior)

demonstrated that although <50% had clinical signs of heart failure, all had anatomic evidence of cardiac dysfunction at autopsy.²¹ Strain abnormalities can help with risk stratification; in patients with RACD undergoing surgery, LV GLS lower than –14.5% predicted worse outcome.²²

Effects of Radiotherapy and Chemotherapy

In patients receiving chemotherapy, an early decline in GLS has been associated with later deterioration in LVEF.²³ Indeed, GLS is incorporated in current clinical guidelines for cardiac monitoring during chemotherapy, particularly anthracyclines²⁴; a reduction of >15% in GLS compared with baseline demonstrates chemotherapy-related cardiotoxicity.²⁴

Table 4. Estimated Rate of Within-Patient Percentage Deterioration from Baseline Strain at 6 Weeks and 12 Months Per Unit Increase in \log_2 (radiation dose) by Region and Across All 18 AHA Segments

Region	6 wks				12 mo			
	Slope	(95% CI)	P Value	P Value Region by \log_2 (Radiation) Interaction	Slope	(95% CI)	P Value	P Value Region by \log_2 (Radiation) Interaction
Basal	–5.6%	(–8.3% to –2.8%)	<0.001	0.373	–4.0%	(–8.4% to 0.5%)	0.079	0.249
Mid	–7.6%	(–9.4% to –5.9%)	<0.001	...	–3.8%	(–6.3% to –1.2%)	0.003	...
Apical	–7.0%	(–8.5% to –5.5%)	<0.001	...	–6.1%	(–8.1% to –4.0%)	<0.001	...
Overall (18 segments)	–5.7%	(–6.4% to –5.0%)	<0.001	...	–4.4%	(–5.3% to –3.5%)	<0.001	...

The slope is the within-patient reduction in the percentage change in strain from baseline associated with a doubling of the radiation dose. AHA indicates American Heart Association.

A 15% reduction in GLS was also reported in 27% of chemotherapy-naïve patients who received radiotherapy,²⁵ and >20% reduction in GLS was observed in 15% of patients.¹²

Because many patients with cancer receive chemotherapy and adjuvant radiotherapy, their synergistic effects would enhance cardiotoxicity. In a large cohort study of childhood cancer survivors, almost one third had altered LV GLS and 11% diastolic dysfunction, both observed with greater frequency in those receiving both chemotherapy and chest radiotherapy.²⁶

Radiotherapy Effects on Global and Segmental Strain

A modest correlation has been demonstrated between mean heart dose of radiotherapy and percent change in LV GLS.¹² In a previous study, patients with breast cancer who received radiotherapy doses >20 Gy to LV volume >15% demonstrated greater reduction in LV GLS.²⁷

Our group and others have demonstrated that the LV apical regions^{8,15} and anterior and anteroseptal walls^{8,15,16} receive the highest radiotherapy dose with tangential radiotherapy for breast cancer. While this is intuitive (ie, that the spatial location of the heart means that the apical anterior segments are in closest proximity to the radiotherapy beam), in this study we could establish, for the first time, a dose–response relationship between segmental LV percentage deterioration from baseline strain at 6 weeks and 12 months with segmental radiotherapy dose received.

Pathophysiology of Radiotherapy-Induced Myocardial Dysfunction

The mechanism of radiotherapy-induced injury to cardiac muscle remains unclear. Our study suggests that the extent of myocardial dysfunction is related to both the dosimetric and spatial effects of radiotherapy. The greatest reduction in segmental strain occurred acutely, within the first 6 weeks postradiotherapy. Early changes postradiotherapy include myocyte injury and loss of endothelial cells with associated inflammation, tissue edema, and vascular damage,²⁸ with resultant alteration in strain. Eventually, radiotherapy-induced fibrosis occurs as a reparative response of the heart tissue to microvascular injury,²⁹ and long-term attenuation in the segmental strain (at 12 months) likely reflects this reparative remodeling. However, persisting alterations at 12 months is a key point that may be clinically relevant in the long-term management, especially in patients receiving chemotherapy.

Dose–Response Relationship

Our study reports a definite dose–response relationship between radiotherapy dose and impaired

segmental strain, evident even at 12 months. Previous studies have largely reported correlation between radiation dose to cardiac structures, particularly focused on coronary artery disease,⁴ as long-term outcomes (>10 years) after radiotherapy. A linear relationship between radiation dose and late major coronary events has been shown, with an increased relative risk of 7.4% seen with each additional unit of radiation, up to 20 years postradiotherapy.⁴ We demonstrated impairment in strain in the short- to medium-term, which implies that subclinical cardiac dysfunction because of RACD appears long before the onset of clinically significant cardiac events.

Contemporary Techniques to Minimize Cardiac Radiation

Our study illustrates the need to explore techniques to reduce RACD, including cardiac autosegmentation use in radiotherapy treatment planning for dose modification for those patients with high dose,³⁰ as well as techniques such as deep inspiration breath hold and intensity-modulated radiotherapy.⁷ Deep inspiration breath hold takes advantage of a more favorable position of the heart during inspiration to minimize heart doses, with benefit in patients with left-sided breast cancer receiving locoregional nodal irradiation.⁷ Other techniques including prone positioning and proton beam radiotherapy⁷ are cardiac sparing, as reported in a recent multicenter study.³¹

Clinical Implications

The most relevant finding of our study is the approximately linear within-patient dose–response relationship between \log_2 (radiotherapy dose) and percent reduction from baseline in segmental strain. A reduction in GLS is predictive of future cardiac failure in the setting of chemotherapy,²³ and in a recent meta-analysis, almost 16% of patients exposed to ionizing radiation developed heart failure.³² This study examined only patients undergoing tangential beam radiotherapy; one of the challenges for breast cancer is the emerging benefit from regional nodal radiotherapy, which may result in greater cardiac doses.

Early identification of patients at risk, and appropriate commencement of cardioprotective therapy, could prevent development of overt RACD, indicating the potential role of myocardial strain imaging in ongoing surveillance of these patients.

LIMITATIONS

The modest sample size was a limitation; however, given the specific eligibility criteria, this represents a good number. Because previous studies in patients with right-sided breast cancer receiving radiotherapy

have demonstrated extremely low heart radiotherapy dose, and no change in strain (including apical strain) early after and up to 3 years postradiotherapy,^{17,25} we did not include a control group of patients who received no radiotherapy. A study with longer follow-up would allow our results to be validated and facilitate correlation of reduced LV GLS with long-term adverse outcomes. The doses reported throughout this article are doses as predicted by the treatment planning system based on routine clinical practice in all patients receiving radiotherapy. Prescribed and received doses can vary because of a range of uncertainties including patient set-up, patient movement, etc. However, planned dose is the most optimal manner in which dose received can be approximated, and all studies to date analyzing dose effect for radiotherapy and the heart use this same parameter. Another limitation is that we did not use autosegmentation or four-dimensional computed tomography, because this is not routinely utilized in clinical practice for breast cancer quantification. Finally, we did not evaluate the impact of radiation dose on specific cardiac structures (eg, coronary arteries), which usually occurs late.

CONCLUSIONS

In patients with left-sided breast cancer undergoing radiotherapy, apical segments, and anterior, anteroseptal, and anterolateral LV walls receive the greatest radiotherapy dose, and consequently are associated with the largest reduction in myocardial strain, demonstrated up to 12 months postradiotherapy. Longer-term studies are required in larger patient groups to determine the prognostic value of these findings as a marker for future adverse cardiac events.

ARTICLE INFORMATION

Received September 21, 2020; accepted January 29, 2021.

Affiliations

From the Department of Cardiology, Westmead Hospital, Sydney, NSW, Australia (S.J.T., L.S., L.T.); Westmead Clinical School, University of Sydney, NSW, Australia (S.J.T., L.T.); South Western Sydney Clinical School, University of New South Wales, Sydney, NSW, Australia (S.T., Q.L., J.O., M.J., V.B., L.H., G.P.D., E.K., L.T.); Ingham Institute of Applied Medical Research, Sydney, NSW, Australia (S.T., M.J., V.B., L.H., G.P.D., E.K.); Central Coast Cancer Therapy Centre, Gosford, NSW, Australia (S.T.); Research and Education Network, Western Sydney Local Health District, Westmead Hospital, Sydney, NSW, Australia (K.B.); NHMRC Clinical Trials Centre, University of Sydney, NSW, Australia (K.B.); Department of Cardiology, St George Hospital, Sydney, NSW, Australia (Q.L.); Department of Cardiology (J.O., D.T.) and Cancer Therapy Centre, Liverpool Hospital, Sydney, NSW, Australia (M.J., V.B., L.H., G.P.D., E.K.).

Sources of Funding

None.

Disclosures

None.

REFERENCES

- Bray F, Ferlay J, Soerjomataram I, Siegel RL, Torre LA, Jemal A. Global cancer statistics 2018: GLOBOCAN estimates of incidence and mortality worldwide for 36 cancers in 185 countries. *CA Cancer J Clin*. 2018;68:394–424. DOI: 10.3322/caac.21492.
- McGale P, Taylor C, Correa C, Cutter D, Duane F, Ewertz M, Gray R, Mannu G, Peto R, Whelan T, et al. Effect of radiotherapy after mastectomy and axillary surgery on 10-year recurrence and 20-year breast cancer mortality. *Lancet*. 2014;383:2127–2135.
- Delaney G, Barton M, Jacob S. Estimation of an optimal radiotherapy utilization rate for breast carcinoma. *Cancer*. 2003;98:1977–1986. DOI: 10.1002/cncr.11740.
- Darby SC, Ewertz M, McGale P, Bennet AM, Blom-Goldman U, Brønnum D, Correa C, Cutter D, Gagliardi G, Gigante B, et al. Risk of ischemic heart disease in women after radiotherapy for breast cancer. *N Engl J Med*. 2013;368:987–998. DOI: 10.1056/NEJMoa1209825.
- Desai MY, Windecker S, Lancellotti P, Bax JJ, Griffin BP, Cahlon O, Johnston DR. Prevention, diagnosis, and management of radiation-associated cardiac disease: JACC scientific expert panel. *J Am Coll Cardiol*. 2019;74:905–927.
- Trivedi SJ, Altman M, Stanton T, Thomas L. Echocardiographic strain in clinical practice. *Heart Lung Circ*. 2019;28:1320–1330. DOI: 10.1016/j.hlc.2019.03.012.
- Bergom C, Currey A, Desai N, Tai A, Strausz JB. Deep inspiration breath hold: techniques and advantages for cardiac sparing during breast cancer irradiation. *Front Oncol*. 2018;8:87. DOI: 10.3389/fonc.2018.00087.
- Tang S, Otton J, Holloway L, Delaney GP, Liney G, George A, Jameson M, Tran D, Batumalai V, Thomas L, et al. Quantification of cardiac sub-volume dosimetry using a 17 segment model of the left ventricle in breast cancer patients receiving tangential beam radiotherapy. *Radiother Oncol*. 2019;132:257–265. DOI: 10.1016/j.radonc.2018.09.021.
- Lang RM, Bierig M, Devereux RB, Flachskampf FA, Foster E, Pellikka PA, Picard MH, Roman MJ, Seward J, Shanewise J, et al. Recommendations for chamber quantification. *Eur J Echocardiogr*. 2006;7:79–108. DOI: 10.1016/j.euje.2005.12.014.
- Feng M, Moran JM, Koelling T, Chughtai A, Chan JL, Freedman L, Hayman JA, Jaggi R, Jolly S, Larouere J, et al. Development and validation of a heart atlas to study cardiac exposure to radiation following treatment for breast cancer. *Int J Radiat Oncol Biol Phys*. 2011;79:10–18. DOI: 10.1016/j.ijrobp.2009.10.058.
- Duane F, Aznar MC, Bartlett F, Cutter DJ, Darby SC, Jaggi R, Lorenzen EL, McArdle O, McGale P, Myerson S, et al. A cardiac contouring atlas for radiotherapy. *Radiother Oncol*. 2017;122:416–422. DOI: 10.1016/j.radonc.2017.01.008.
- Lo Q, Hee L, Batumalai V, Allman C, MacDonald P, Delaney GP, Lonergan D, Thomas L. Subclinical cardiac dysfunction detected by strain imaging during breast irradiation with persistent changes 6 weeks after treatment. *Int J Radiat Oncol Biol Phys*. 2015;92:268–276. DOI: 10.1016/j.ijrobp.2014.11.016.
- Sritharan HP, Delaney GP, Lo Q, Batumalai V, Xuan W, Thomas L. Evaluation of traditional and novel echocardiographic methods of cardiac diastolic dysfunction post radiotherapy in breast cancer. *Int J Cardiol*. 2017;243:204–208. DOI: 10.1016/j.ijcard.2017.05.007.
- Trivedi SJ, Choudhary P, Lo Q, Sritharan HP, Iyer A, Batumalai V, Delaney GP, Thomas L. Persistent reduction in global longitudinal strain in the longer term after radiation therapy in patients with breast cancer. *Radiother Oncol*. 2019;132:148–154. DOI: 10.1016/j.radonc.2018.10.023.
- Lo Q, Hee L, Batumalai V, Allman C, MacDonald P, Lonergan D, Delaney GP, Thomas L. Strain imaging detects dose-dependent segmental cardiac dysfunction in the acute phase after breast irradiation. *Int J Radiat Oncol Biol Phys*. 2017;99:182–190. DOI: 10.1016/j.ijrobp.2017.05.030.
- Erven K, Florian A, Slagmolen P, Sweldens C, Jurcut R, Wildiers H, Voigt JU, Weltens C. Subclinical cardiotoxicity detected by strain rate imaging up to 14 months after breast radiation therapy. *Int J Radiat Oncol Biol Phys*. 2013;85:1172–1178. DOI: 10.1016/j.ijrobp.2012.09.022.
- Tuohinen SS, Skytta T, Poutanen T, Huhtala H, Virtanen V, Kellokumpu-Lehtinen PL, Raatikainen P. Radiotherapy-induced global and regional differences in early-stage left-sided versus right-sided breast cancer patients: speckle tracking echocardiography study. *Int J Cardiovasc Imaging*. 2017;33:463–472. DOI: 10.1007/s10554-016-1021-y.
- Erven K, Jurcut R, Weltens C, Giusca S, Ector J, Wildiers H, Van den Bogaert W, Voigt JU. Acute radiation effects on cardiac function

- detected by strain rate imaging in breast cancer patients. *Int J Radiat Oncol Biol Phys*. 2011;79:1444–1451. DOI: 10.1016/j.ijrobp.2010.01.004.
19. Heggemann F, Grotz H, Welzel G, Dösch C, Hansmann J, Kraus-Tiefenbacher U, Attenberger U, Schönberg SO, Borggreffe M, Wenz F, et al. Cardiac function after multimodal breast cancer therapy assessed with functional magnetic resonance imaging and echocardiography imaging. *Int J Radiat Oncol Biol Phys*. 2015;93:836–844. DOI: 10.1016/j.ijrobp.2015.07.2287.
 20. Kalam K, Otahal P, Marwick TH. Prognostic implications of global lv dysfunction: a systematic review and meta-analysis of global longitudinal strain and ejection fraction. *Heart*. 2014;100:1673–1680. DOI: 10.1136/heartjnl-2014-305538.
 21. Brosius FC 3rd, Waller BF, Roberts WC. Radiation heart disease. Analysis of 16 young (aged 15 to 33 years) necropsy patients who received over 3,500 rads to the heart. *Am J Med*. 1981;70:519–530.
 22. Chirakarnjanakorn S, Popović ZB, Wu W, Masri A, Smedira NG, Lytle BW, Griffin BP, Desai MY. Impact of long-axis function on cardiac surgical outcomes in patients with radiation-associated heart disease. *J Thorac Cardiovasc Surg*. 2015;149:e1642. DOI: 10.1016/j.jtcvs.2015.01.045.
 23. Guerra F, Marchesini M, Contadini D, Menditto A, Morelli M, Piccolo E, Battelli N, Pistelli M, Berardi R, Cascinu S, et al. Speckle-tracking global longitudinal strain as an early predictor of cardiotoxicity in breast carcinoma. *Support Care Cancer*. 2016;24:3139–3145. DOI: 10.1007/s00520-016-3137-y.
 24. Plana JC, Galderisi M, Barac A, Ewer MS, Ky B, Scherrer-Crosbie M, Ganame J, Sebag IA, Agler DA, Badano LP, et al. Expert consensus for multimodality imaging evaluation of adult patients during and after cancer therapy: a report from the American society of echocardiography and the European association of cardiovascular imaging. *Eur Heart J Cardiovasc Imaging*. 2014;15:1063–1093. DOI: 10.1016/j.echo.2014.07.012.
 25. Tuohinen SS, Skytta T, Huhtala H, Virtanen V, Kellokumpu-Lehtinen PL, Raatikainen P. Left ventricular speckle tracking echocardiography changes among early-stage breast cancer patients three years after radiotherapy. *Anticancer Res*. 2019;39:4227–4236. DOI: 10.21873/anticancer.13584.
 26. Armstrong GT, Joshi VM, Ness KK, Marwick TH, Zhang N, Srivastava D, Griffin BP, Grimm RA, Thomas J, Phelan D, et al. Comprehensive echocardiographic detection of treatment-related cardiac dysfunction in adult survivors of childhood cancer: results from the St. Jude lifetime cohort study. *J Am Coll Cardiol*. 2015;65:2511–2522. DOI: 10.1016/j.jacc.2015.04.013.
 27. Walker V, Lairez O, Fondard O, Pathak A, Pinel B, Chevelle C, Franck D, Jimenez G, Camilleri J, Panh L, et al. Early detection of subclinical left ventricular dysfunction after breast cancer radiation therapy using speckle-tracking echocardiography: association between cardiac exposure and longitudinal strain reduction (BACCARAT study). *Radiat Oncol*. 2019;14:204. DOI: 10.1186/s13014-019-1408-8.
 28. Stewart FA, Hoving S, Russell NS. Vascular damage as an underlying mechanism of cardiac and cerebral toxicity in irradiated cancer patients. *Radiat Res*. 2010;174:865–869. DOI: 10.1667/RR1862.1.
 29. Schultz-Hector S, Trott KR. Radiation-induced cardiovascular diseases: Is the epidemiologic evidence compatible with the radiobiologic data? *Int J Radiat Oncol Biol Phys*. 2007;67:10–18. DOI: 10.1016/j.ijrobp.2006.08.071.
 30. Finnegan R, Dowling J, Koh ES, Tang S, Otton J, Delaney G, Batumalai V, Luo C, Atluri P, Satchithanandha A, et al. Feasibility of multi-atlas cardiac segmentation from thoracic planning CT in a probabilistic framework. *Phys Med Biol*. 2019;64:085006. DOI: 10.1088/1361-6560/ab0ea6.
 31. Pierce LJ, Feng M, Griffith KA, Jagsi R, Boike T, Dryden D, Gustafson GS, Benedetti L, Matuszak MM, Nurushev TS, et al. Recent time trends and predictors of heart dose from breast radiation therapy in a large quality consortium of radiation oncology practices. *Int J Radiat Oncol Biol Phys*. 2017;99:1154–1161. DOI: 10.1016/j.ijrobp.2017.07.022.
 32. Cheng Y-J, Nie X-Y, Ji C-C, Lin X-X, Liu L-J, Chen X-M, Yao H, Wu S-H. Long-term cardiovascular risk after radiotherapy in women with breast cancer. *J Am Heart Assoc*. 2017;6:e005633. DOI: 10.1161/JAHA.117.005633.